Jour. Fac. Sci., Hokkaido Univ., Ser. VII (Geophysics), Vol. 8, No. 3, 221-241, 1988.

Numerical Study on the Seasonal Variation of the Cold Water Tongue in the Eastern Tropical Pacific

Kensuke Takeuchi

Department of Geophysics, Faculty of Science, Hokkaido University, Sapporo 060, Japan

(Received Nov. 11, 1987)

Abstract

In an attempt to throw light on the mechanisms behind the seasonal variation of the cold water tongue in the eastern tropical Pacific Ocean, a numerical modelling study is carried out using a 10-level model with a rectangular flat-bottomed model ocean. A Haney type sea surface heat flux formulation and Richardson number dependent vertical mixing coefficients are used in the model. The seasonal variation of wind stress is idealized as a seasonal north-south migration of a trade wind system, while the thermal boundary condition is fixed.

The model succeeds in reproducing a cold water tongue which develops from northern summer to fall and shrinks from winter to spring ; similar to the characteristics of the observed tongue. Various analyses of the model results indicate the seasonal evolution of the cold water tongue is as follows. In southern winter, stronger equatorward wind stress along the eastern boundary south of the equator enhances coastal upwelling there. In addition to this loacal upwelling, upwelling Kelvin waves, generated by an increase of the easterly wind stress along the equator, inpinging upon the eastern bokndary from southern winter to spring. The upwelled cold water is advected equatorward and then westward along the equator by the westward surface current which is coincidently stronger due to the upwelling Kelvin waves, resulting in the development of a cold water tongue in southern winter to spring.

1. Introduction

It is widely known that in the El Nino years, sea-surface temperature in the eastern equatorial Pacific zone becomes anomalously higher than usual by up to several degrees centigrade. We must note, however, this does not mean that SST in the region is necessarily higher than the surrounding area. Usually during non El Nino conditions, SST in the region is distinctly lower than the surrounding area, forming a cold water tongue which extends several thousand

kilometers along thc Equator west from the South American coast (Robinson, 1976). During El Nino events, the cold tongue weakens or nearly disappears, depending on the magnitude of the events, and the anomalously high SST is the consequence of the weakening of the cold water tongue.

It is also known that the cold tongue repeatedly developes and shrinks seasonally, strongest in the season from late northern summer to early fall and weakest from late winter to early spring. As the SST anomaly in the El Nino events strongly depends on the usually existing cold water tongue, its seasonal variation is an important factor for the evolution of SST anomaly of El Nino events, as is pointed out by Harrison and Schopf (1984). This suggests the importance of determing the mechanisms responsible for the seasonal variation of the cold water necessary for understanding the evolution of the SST anomaly in El Nino events, However overshadowed by interannual variability like EI Nino events the seasonal variation of the Equatorial Pacific SST has been somewhat overlooked.

The present work is an attempt to throw light upon the mechanisms of the seasonal variation of the Equatorial Pacific SST, especially the seasonal evolution of the cold water tongue. For this purpose, a numerical modelling study of the Equatorial Pacific is carried out. The model has been designed to reproduce the main features of the seasonal variation of the cold tongue, the results from which will be used to analyze the mechanisms of the seasonal variation.

2. Model descriptions

The model ocean is a close rectangular basin centered on the equator, 12,000 and 24,000 km wide in the zonal and meridional directions, respectively, with a flat bottom of 4,900 m depth. It is a Bryan type 10-level primitive equation model (Bryan, 1969), with horizontal grid spans of 80 km in both directions and the vertical grid distribution given in Table 1. The vertical resolution of the deeper ocean is largely sacrificed in favor of better resolution in the upper ocean.

Cartesian coordinates are used to describe the governing equations shown below. The model is based on the hydrostatic, Boussinesq, rigid-lid and equatorial β-plane approximations.

$$\frac{\partial u}{\partial t}+\vec{v}\nabla u-\beta yv=-\frac{\partial p}{\partial x}+A_H\left(\frac{\partial^2 u}{\partial x^2}+\frac{\partial^2 u}{\partial y^2}\right)+\frac{\partial}{\partial z}\left(Av\frac{\partial u}{\partial z}\right) \tag{1}$$

$$\frac{\partial v}{\partial t}+\vec{v}\nabla v+\beta yu=-\frac{\partial p}{\partial y}+A_H\left(\frac{\partial^2 v}{\partial x^2}+\frac{\partial^2 v}{\partial y^2}\right)+\frac{\partial}{\partial z^2}\left(Av\frac{\partial v}{\partial z}\right) \tag{2}$$

Table 1 Notation and values

t	time
x, y, z	eastward, northward and upward distances
$\vec{v}$	velocity vector
u, v, w	eastward, northward and upward velocity
p, ρ, T	pressure, density and temperature
T_0	reference temperature
α	thermal expansion coeficient (3.0×10^{-1} kgm^{-3}K^{-1})
β	meridional gradient of Coriolis parameter (2.0×10^{-11} m^{-1}sec^{-1})
g	acceleration of gravity (9.8 msec^{-2})
A_H, K_H	horizontal eddy viscosity and diffusivity coefficeints (2.0×10^{3}, 2.0×10^{2} m^{2}sec^{-1})
A_v, K_v	vertical eddy viscosity and diffusivity coefficient (Eq. 7, 8)
R_i	Richardson number (Eq. 9)
Q	sea surface heat flux
c	coefficient of surface heat flux (23.9 Wm^{-2}K)
T_a	thermal equiliblium temperature
T_s	temperature in the surface layer
C_p	specific heat

$$\frac{\partial u}{\partial x}+\frac{\partial v}{\partial y}+\frac{\partial v}{\partial z}=0 \tag{3}$$

$$\frac{\partial T}{\partial t}+\vec{v}\,\nabla\, T=K_H\left(\frac{\partial^2 T}{\partial x^2}+\frac{\partial^2 T}{\partial y^2}\right)+\frac{\partial}{\partial t}\left(Kv\frac{\partial T}{\partial z}\right) \tag{4}$$

Table 2 Thickness and center depth of each model layer

Layer	Thickness	Depth
1	30 m	15 m
2	30	45
3	30	75
4	30	105
5	30	135
6	50	175
7	90	245
8	150	365
9	550	715
10	4,000	2,990

$$\frac{\partial p}{\partial t} = -\rho g \tag{5}$$

$$\rho = 1.0 + a(T - T_0) \tag{6}$$

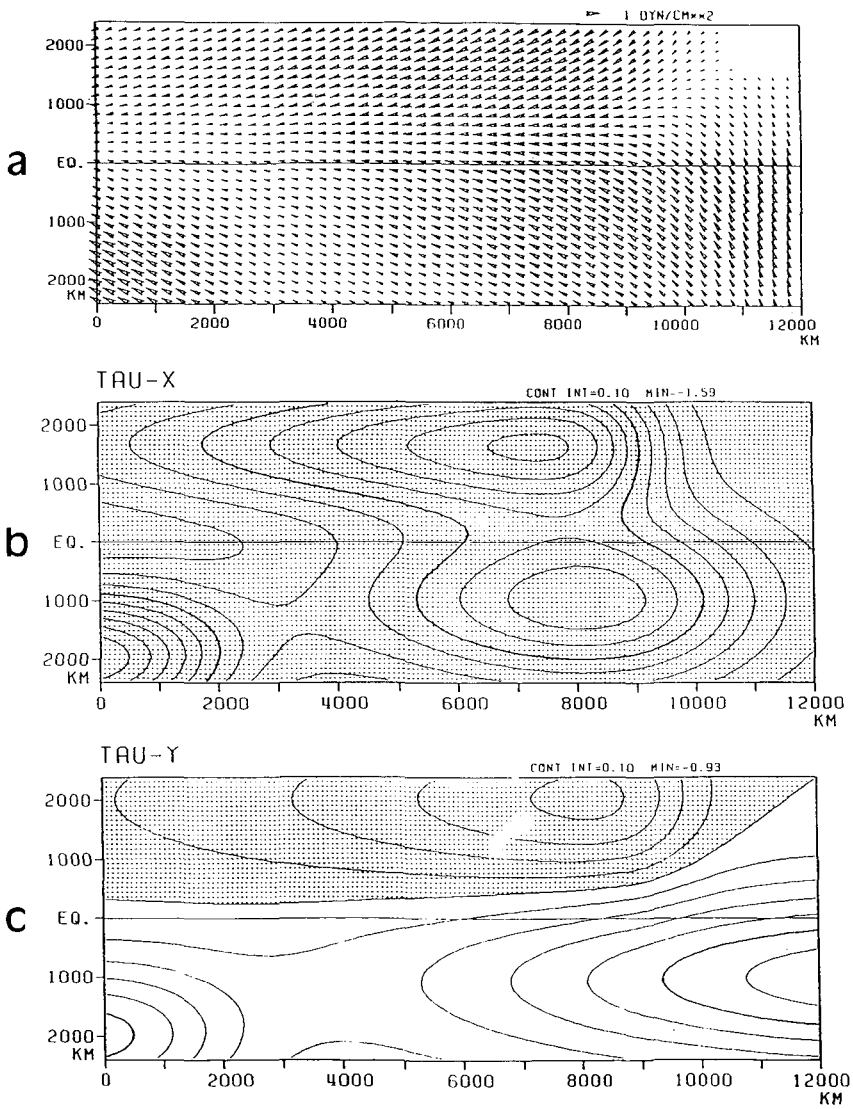

Fig. 1 Distribution of wind stress vector (a), zonal component (b) and meridional component (c) used in the model, at the middle of May and Novenber, when the wind system locates at the mean position.

The symbol notation and the values of the constants are listed in Table 2. Vertical mixings are parameterized by the formulation used in Pakanowski and Philander (1981), as follows.

$$Av=\frac{100.0}{(1.0+5.0\,Ri)^2}+1.0 \tag{7}$$

$$Kv=\frac{Av}{1.0+5.0\,Ri}+0.1 \tag{8}$$

$$Ri=\frac{g\,\partial\rho/\partial z}{\left(\partial u/\partial z\right)^2+\left(\partial v/\partial z\right)^2} \tag{9}$$

Horizontal mixing coefficients are constant in time and space expect in narrow bands adjacent to the northern and southern boundaries where a larger

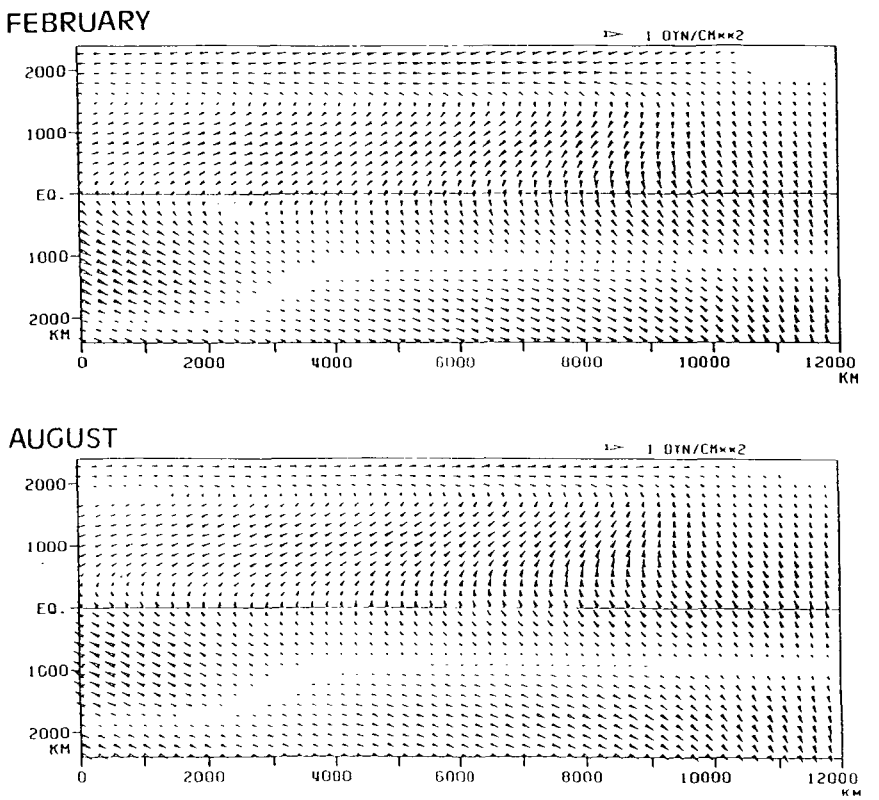

Fig. 2 Departure of the model wind stress at the middle of February and August from the model annual mean.

value is used for a momentum mixing coefficient for the purpose of damping coastal Kelvin waves and preventing a "round trip" of Kelvin waves around the boundaries and the equator.

For surface heat flux, Haney type parameterization is employed (Haney, 1971),

$$Q = c\ (Ta - Ts) \tag{10}$$

where Ts temperature in the surface layer of the model ocean. Ta is kept constant in time and space at 30℃, except for regions adjacent to the northern and southern boundaries where Ta decreases down to around 12℃. The purpose of imposing this cooling region is to allow the model to supply cold water, which otherwise, is not supplied as the model ocean does not include high latitudes region. The four vertical walls and the bottom are adiabatic. Note that there is no seasonal change in thermal condition in the present model.

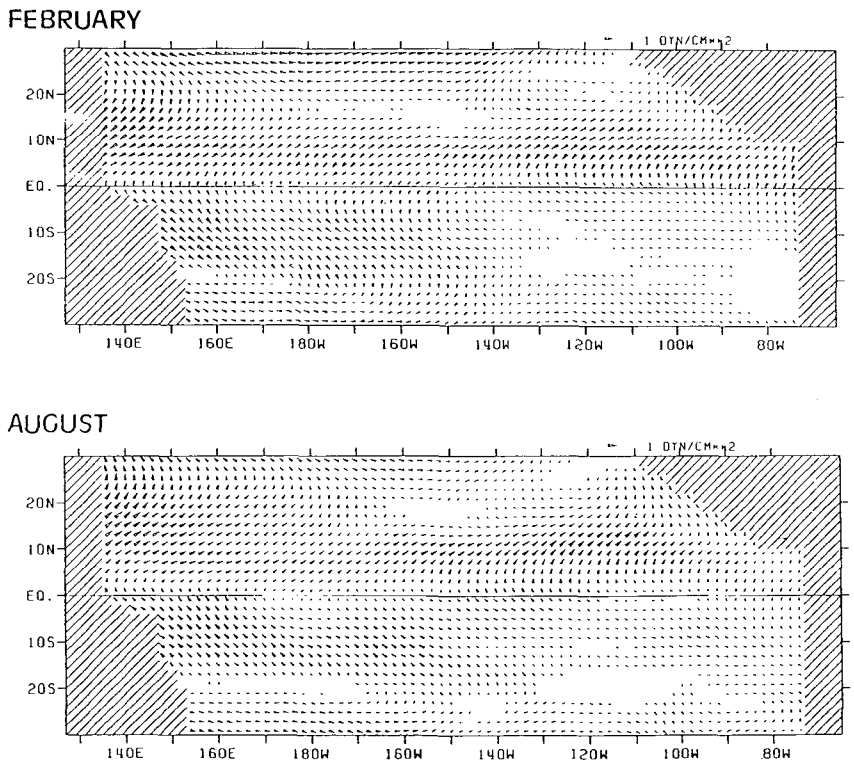

Fig. 3 Observed counterpart of Fig. 2, computed from the FSU wind stress data for 1960-1984 (cf. Goldenberg and O'Brien, 1981).

The only source of seasonal variation of the model ocean is seasonal variations of the wind stress. The wind stress distribution used in the model is an idealized one, in which the seasonal variation is represented as north-south migration of a trade wind system. Fig. 1 shows the wind stress distribution when the wind system is at the mean location (a), its zonal (b) and meridional (c) components. This distribution shifts northward and southward seasonally. The oscillation is sinusoidal with an amplitude of 500 km, and reaches the northern and the southern most location at the middle of February and August, respectively. Fig. 2 shows the model wind stress departure at the middle of February and August from the model annual mean. The similarity of these patterns to the observed patterns from the FSU wind stress data (Goldenberg and O'Brien, 1981) shown in Fig. 3, justifies the use of this model wind stress.

At the initial state, the model ocean is at rest and the stratification is horizontally uniform. Equations (1), (2) and (4) are integrated in time numerically over 7 years, and a quasi-steady periodic state is attained. It is the final one year of the calculation which is shown and analyzed in the following sections.

3. Results of the numerical model

Fig. 4 shows SST distributions in February, May, August and November. A cold water tongue which extends westward along the equator from the eastern boundary of the model ocean can be seen in all seasons. However, strength changes from season to season, which can be seen in the variation of area below 25℃ (shadowed in the figure).

The evolution of the cold tongue can be seen more clearly in the time versus longitude diagrams of temperature at four levels along the equator, shown in Fig. 5. The top panel, which shows the seasonal variation of the model SST along the equator, can be compared to the observed counterpart presented in Fig. 7 of Horel (1982). The model result agree with the observation in the sense that seasonal variations of SST are much larger in the region near the eastern boundary. In the model, the lowest SST near the eastern boundary occurs around August and September and the highest around February, while in the observation, they are around September and March, respectively. The difference between the highest and the lowest observed SST is 4.2℃ and 3.5℃ in Fig. 5. Also, a slight delay in the phase of the seasonal variation of SST increases with distance from the eastern boundary, is common to both figures. The most serious discrepancy is that the clear seasonal cycle can be traced out

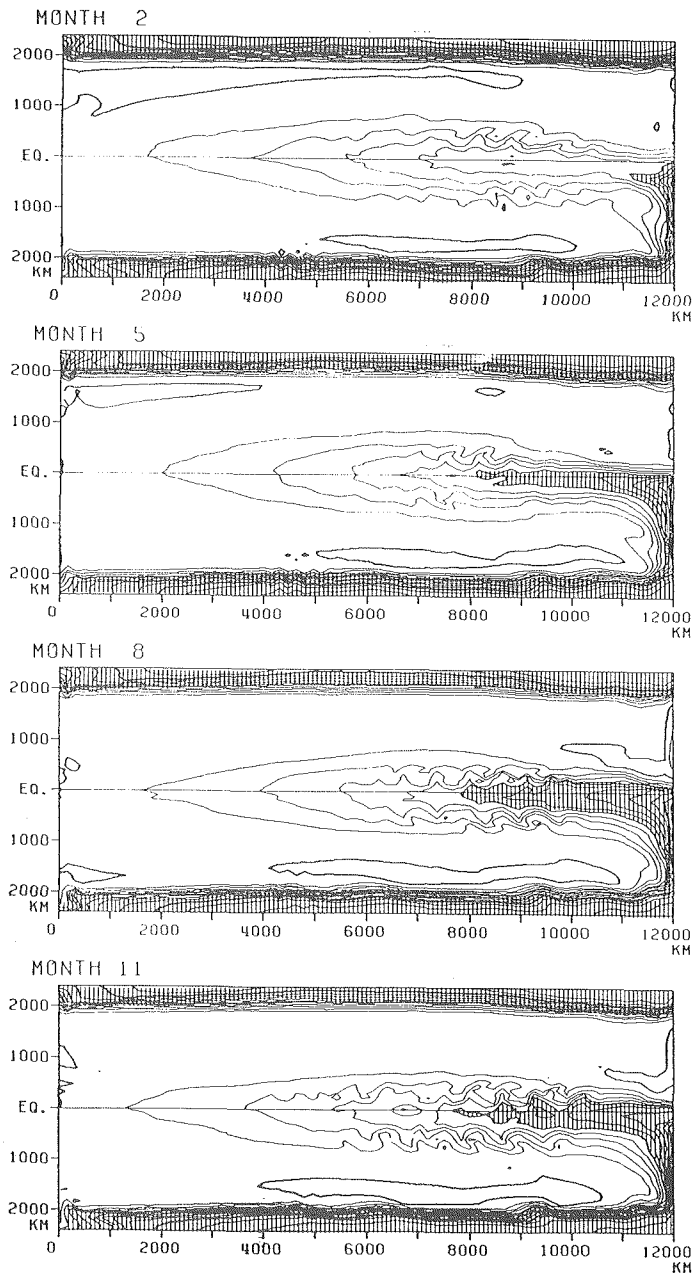

Fig. 4 Horizontal sea-surface temperature (°C) distribution at the middle of, from the top, February, May, August and November, respectively. Areas colder than 25°C are shaded.

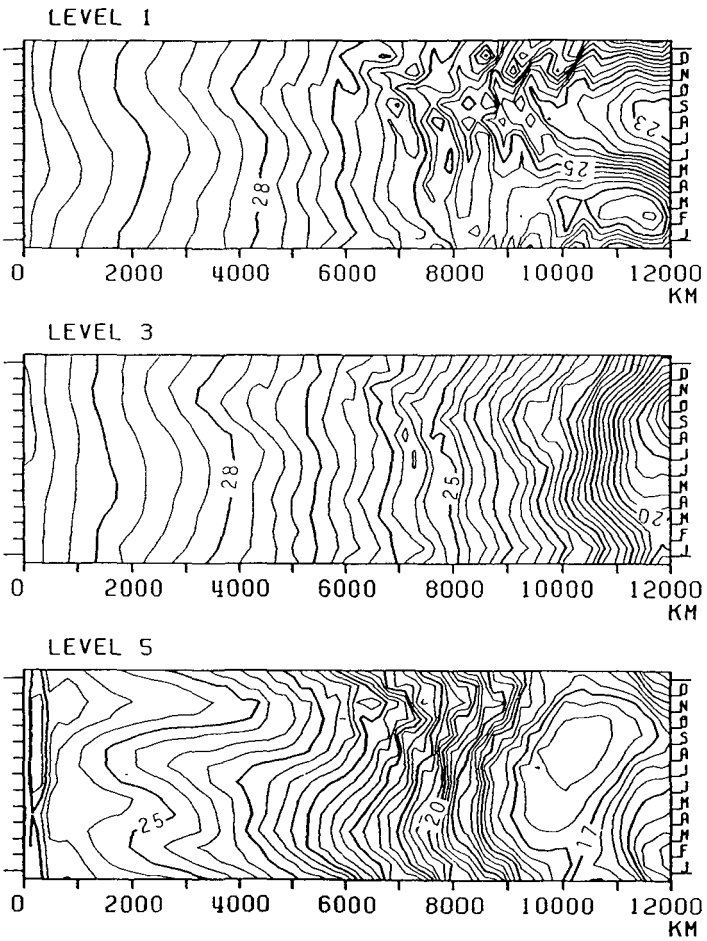

Fig. 5 x-t diagrams of sea-water temperature (°C) at the equator in the upper four layers of the model ocean, for the final one year of the calculation. The contour interval is 0.25°C.

west from the eastern boundary as far as 7,000 km in Horel's figure, while in the model it can be traced only about 4,000 km. However, it can be summed up that the model succeeds in reproducing the main qualitative features of seasonal variation of the cold water tongue. It suggests that the mechanisms of the seasonal variation of the cold tongue in the present model is essentially analogous to the one in the real ocean. Hence it is meaningful to analyze the model result.

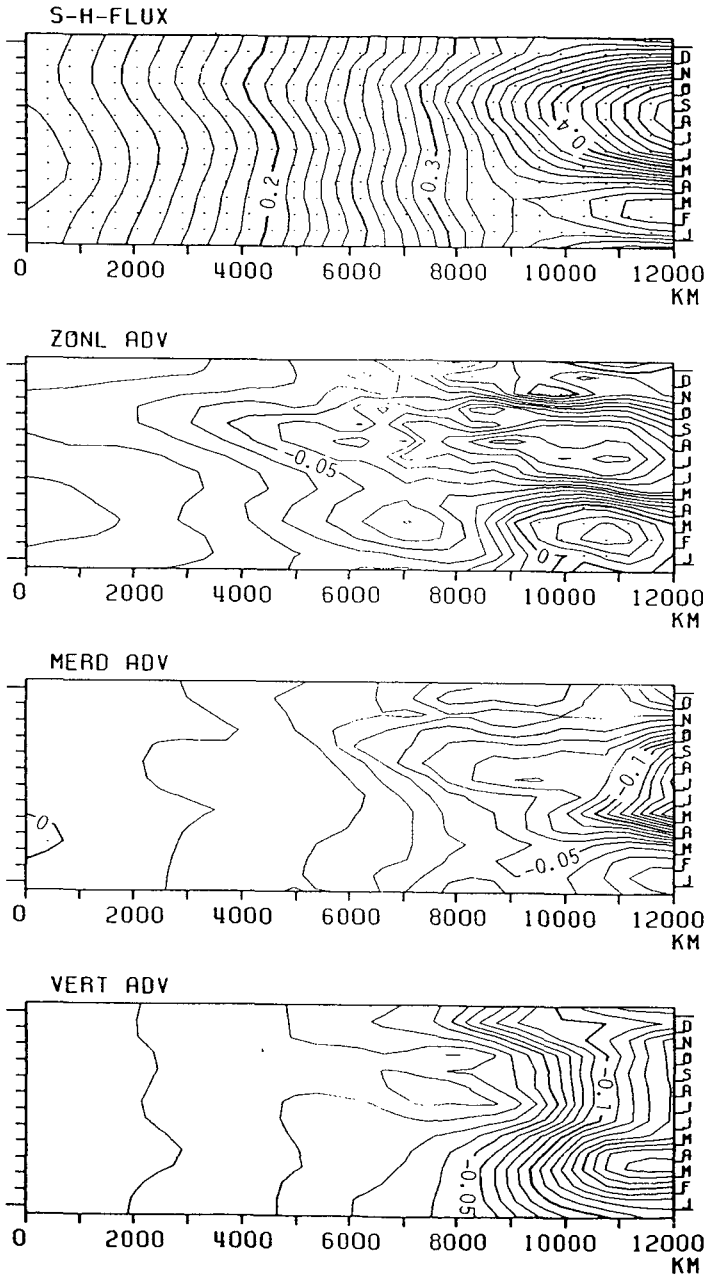

Fig. 6 x-t diagrams of magnitudes of terms in the temperature prediction equation along the equator (°C/month). Shading indicates the term is a warming factor.

4. Analysis of the model result

(a) Relative contribution to SST change

First, contributions of the terms in the SST tendency equation in the model (Eq. 4) along the equator are shown in Fig. 6. Mixing terms, both vertical and lateral, are not shown here, as they are negligibly smaller than the others. The sea surface flux term and vertical advection term are working passively as damping factors of the seasonal variation of SST, as they have negative correlation to the SST change. It should be stressed that a contribution of equatorial upwelling for the seasonal change of the SST is negative. The remaining two terms are responsible for the SST change. The zonal advection term is dominant in most of the area where the seasonal change of SST is strong, while meridional advection is important near the eastern boundary. It suggests the following process of the development of the cold tongue. The origin of the cold water comes from somewhere along the eastern boundary, advected equatorward along the coast and then westward along the equator.

(b) Origin and route of cold water

There are only two possible routes of cold water supply in the model. One is from the cooling region near the pole side boundary via meridional advection, and another is from the depth via upwelling. Although there is some supply of cold water from the cooling region equatorward along the eastern boundary, the amount is too small for the development of the cold tongue. It leaves only one possibility, the coastal upwelling along the eastern boundary.

Fig. 7 shows the seasonal variation of vertical velocity at the bottom of the surface layer (30 m) along the eastern boundary. A strong upwelling region is found between the equator and several hundreds kilometer south of it. The

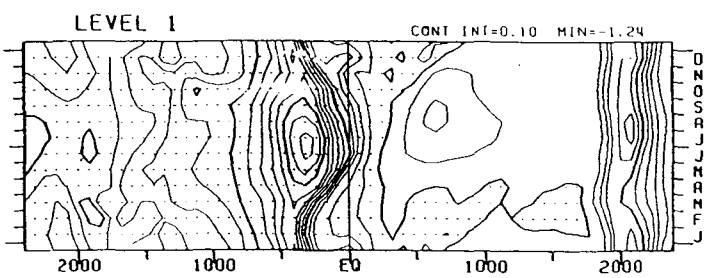

Fig. 7 y-t diagram of vertical velocity at the bottom of the surfcace layer (30 m) along the eastern boundary (contour interval, 1.0×10 cm/sec). Shading indicates upwelling.

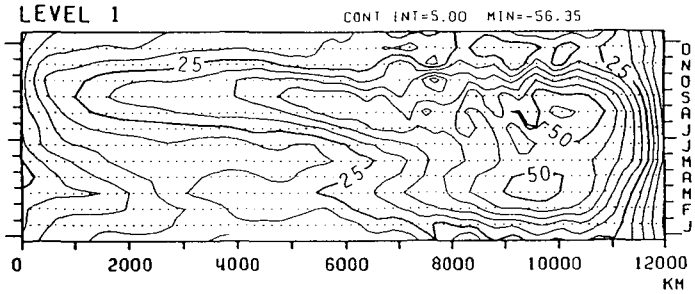

Fig. 8 x-t diagram of surface zonal current (cm/sec) at the equator. Shading means the current is westward.

upwelling intensity there is showing strong seasonal variation, and the strongest season is around June and July. This coincides with the beginning of the development of the cold tongue.

The zonal surface current near the equator is also showing strong seasonal variation as is seen in Fig. 8. In the eastern third portion of the model ocean, where the seasonal variation of SST is strong, there is a prominent semiannual component so that the westward current has two peaks in one year. The season when the cold tongue develops coincides with the one of the peaks, from June to September.

Summarizing the above, the process of the development of the cold water tongue is suggested to be the following. Strong coastal upwelling along the eastern boundary ranging several hundreds of kilometers south of the equator supplies cold water from the deeper ocean in the season centered around June and July. After being advected equatorward, the cold surface water extends westward, carried by a coincidently strong westward current. The westward current spped at the time is around 50 cm/sec, so it takes 2-3 months for the cold water to travel 4,000 km, the length of the area where strong SST seasonal variation can be seen in the model. The time scale in which sea-surface heat flux, formulated as in Eq. 10, heat up the surface layer to the equilibrium temperature Ta is calculated as,

$$\tau = Cp\ \Delta z\rho / C \sim 60 \text{ days} \qquad (11)$$

where Δz is the thickness of the surface layer. The matching of the two time scales supports the idea that the cold water is supplied at the eastern boundary, advected westward while being warmed up by sea-surface heat flux and finally becoming indistinguishable from the surrounding water.

Now, the remaining question is why the coastal upwelling and the westward current are strong at the specific sebsons. As wind stress is the only external forcing changing seasonally, it should be responsible in some way. Eqpecially, the zonal component along the equator and the meridional component along the eastern boundary are considered to be important.

The role of alongshore coastal winds are a rather direct cause of local coastal upwelling. Certainly, equatorward wind stress, which is favorable for

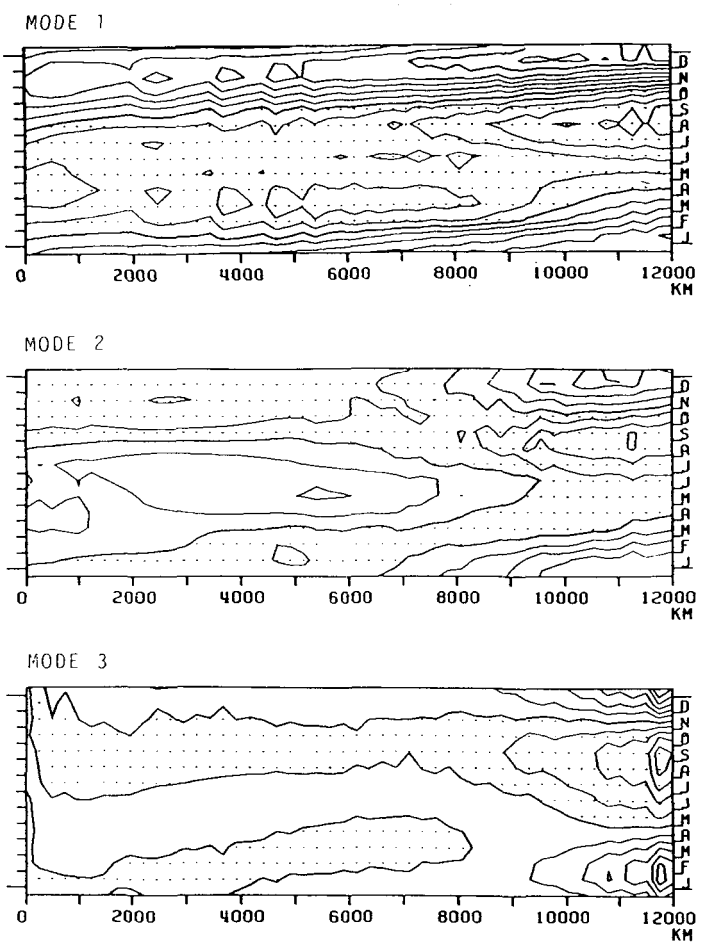

Fig. 9 x-t diagrams of the amplitudes of the gravest three baroclinic mode Kelvin waves. Shading indicates the amplitude is negative, which corresponds to that the Kelvin wave is associated with upwelling near the sea surface and westward surface current.

the coastal upwelling, is strongest in southern winter in the area where strong coastal upwelling takes place in the same season.

On the other hand, effects of zonal wind stress along the equator are not as straight forward. At the same time it enhances or depresses local equatorial upwelling, which is found not important for the development of the cold water tongue, it generates equatorial waves, whose effects are not necessarily local.

(c) Role of remotely forced equatorial Kelvin waves

In order to examine the propagation of equatorial Kelvin waves, decomposition into equatorial modes, both in vertical and meridional, is done. Detailed discussion on the generation and propagation of equatorial waves, along with

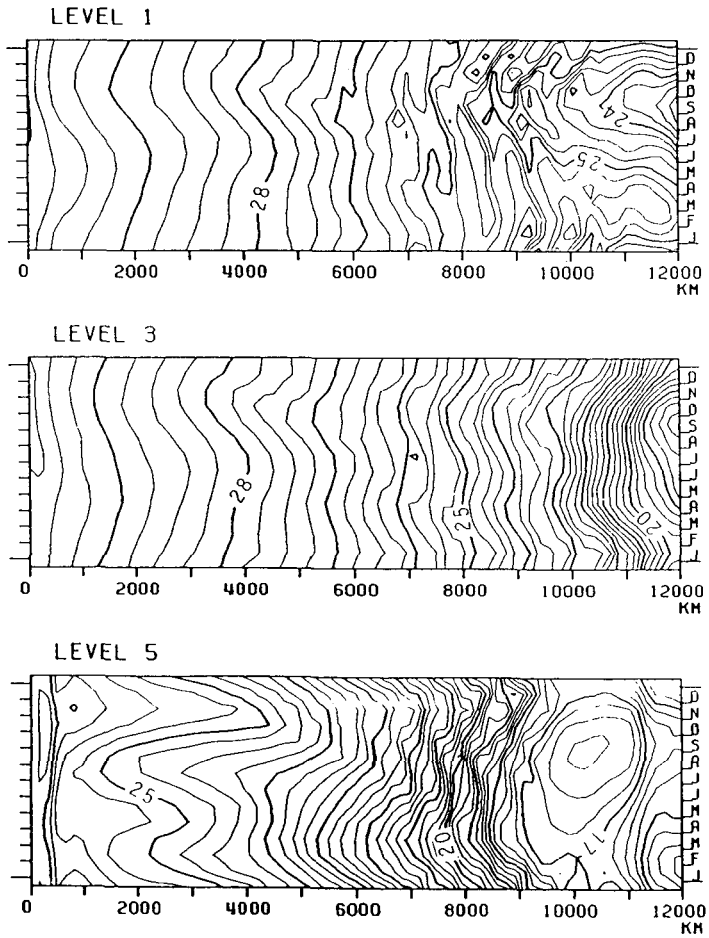

Fig. 10(a) Same as Fig. 5 except for Z model.

the procedure of the decomposition, will appear in another paper (in preparation). Here, only equatorial Kelvin wave mode components of the gravest three baroclinic modes are shown in Fig. 9. Shaded area in the figure indicates vertical motion near the sea surface associated with what is designated an upwelling Kelvin wave. For all three modes, upwelling Kelvin waves reach the eastern boundary from late northern summer to early fall. They are expected to contribute to coastal upwelling along the eastern boundary by pushing up the thermocline there. This yield another possible cause for the enhancement of the coastal upwelling in southern wintertioned earlier.

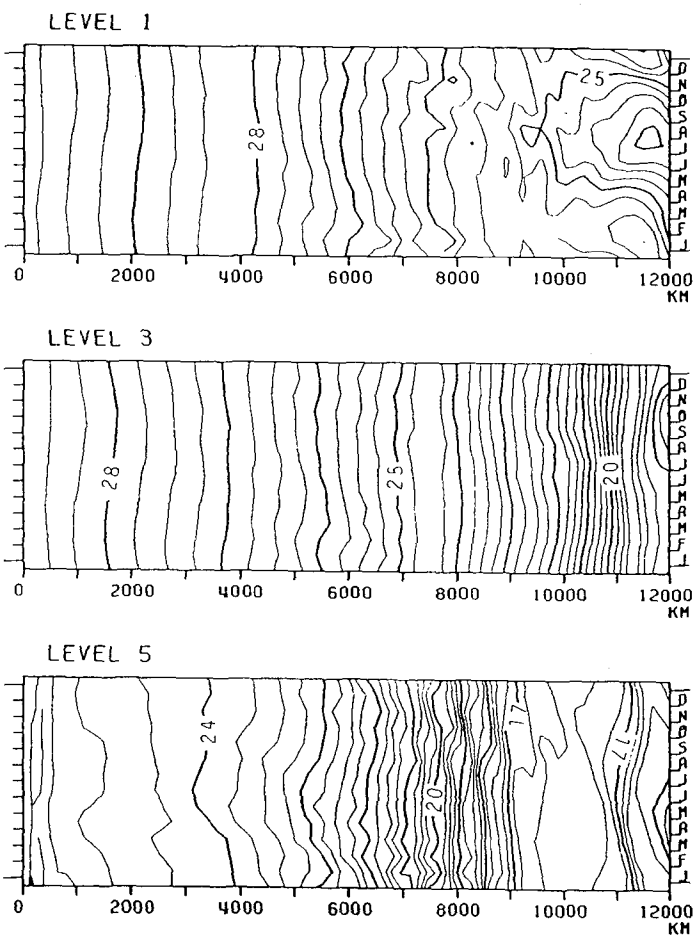

Fig. 10(b) Same as Fig. 5 except for M model.

At the same time, as upwelling Kelvin waves which are associated with westward surface current, are responsible for the strong westward surface current along the equator in the eastern portion of the model ocean (Fig. 8).

(d) Relative importance of local and remote forcing

By the preceeding discussion, it is indicated that the seasonal variation of the cold water tongue is attributed to both variations of locally induced coastal upwelling along the eastern boundary by changing meridinal wind stress and remotely forced equatorial Kelvin waves generated by variation of zonal equatorial wind stress. The remaining problem is to decide their relative importance. For the purpose, two additional model experiments are carried out. In one of them (hereafter, called M model), zonal wind stress is fixed at May condition, when the wind stress system is at the mean location, while meridional compo-

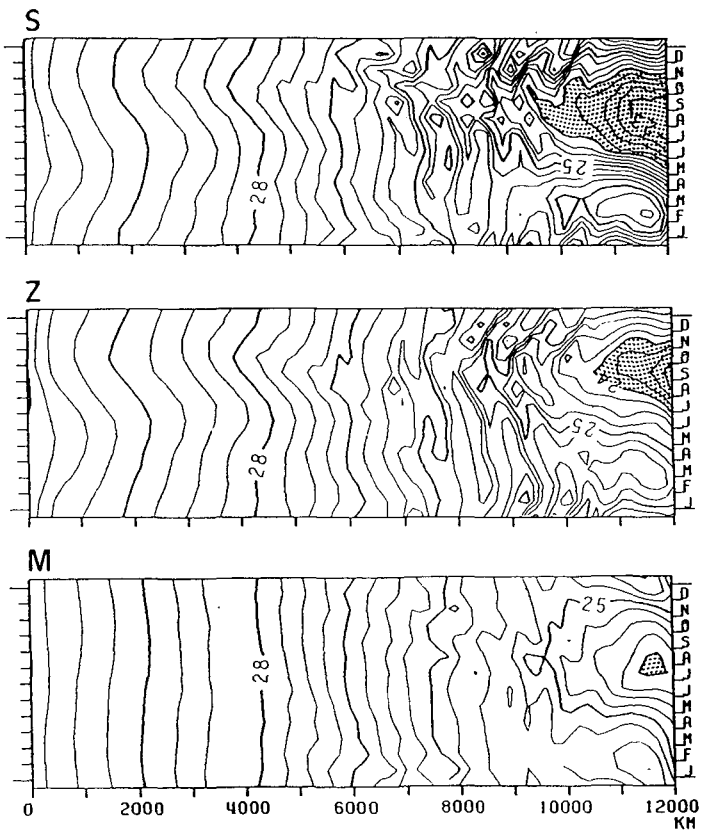

Fig. 11 x-t diagrams of surface zonal current along the equator in the models S, Z and M. Shading indicates that the temperature is colder than 24°C.

nent is changing identically as in the previous model (S model). In the other (Z model), on the contrary, meridional component is fixed and zonal component is changing.

The output of the S model at 2.5 years previous to the end of the calculation is used as the initial condition and then the new models take over the calculation for 2.5 years. Comparison are made for the last one year of each calculation, when the new models each reach their new quasi steady-periodic state.

In Fig. 10, x-t diagrams of temperature at three levels are shown for the Z and M models, which correspond to Fig. 5. In the Z models, except for the surface layer, temperature variations resemble closely to that of the S model.

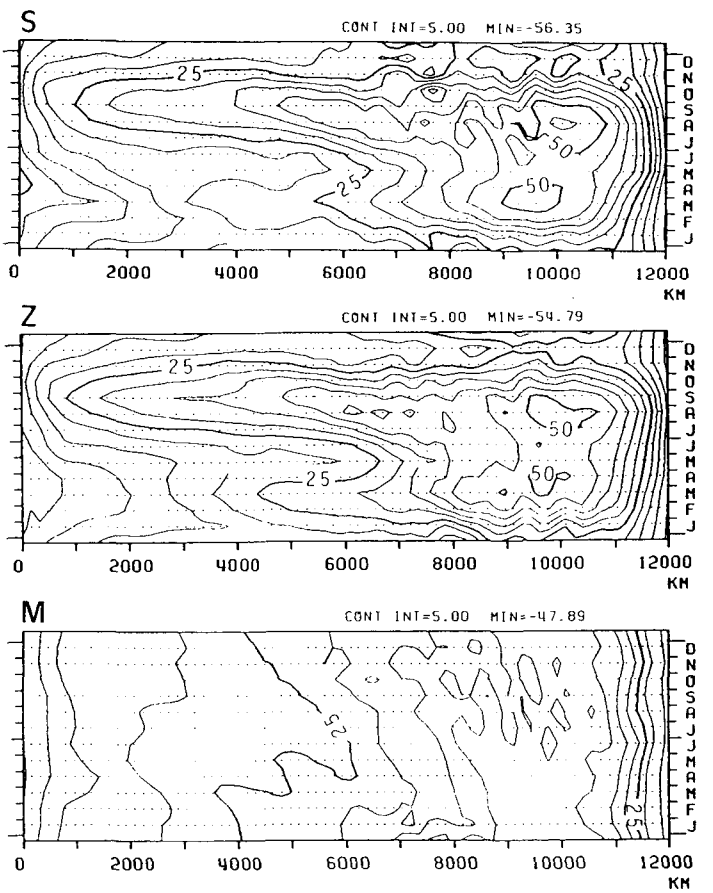

Fig. 12 x-t diagrams of surface zonal current along the equator in Z model and M model compared to S model.

In contrast, variation in deeper ocean in the M model is very small, which indicates that equatorial waves are nearly absent. In both models seasonal variations of SST are apparent, but significantly weaker than in the S model. It is more easily seen Fig. 11, where x-t diagrams of SST of the three models are shown together.

What these figures suggest is that both variation of the zonal and meridional wind stress components contribute to the seasonal variation of the cold tongue. Rough quantitative measures of their relative importance are provided by comparison of the differences between the maximums and minimums in SST

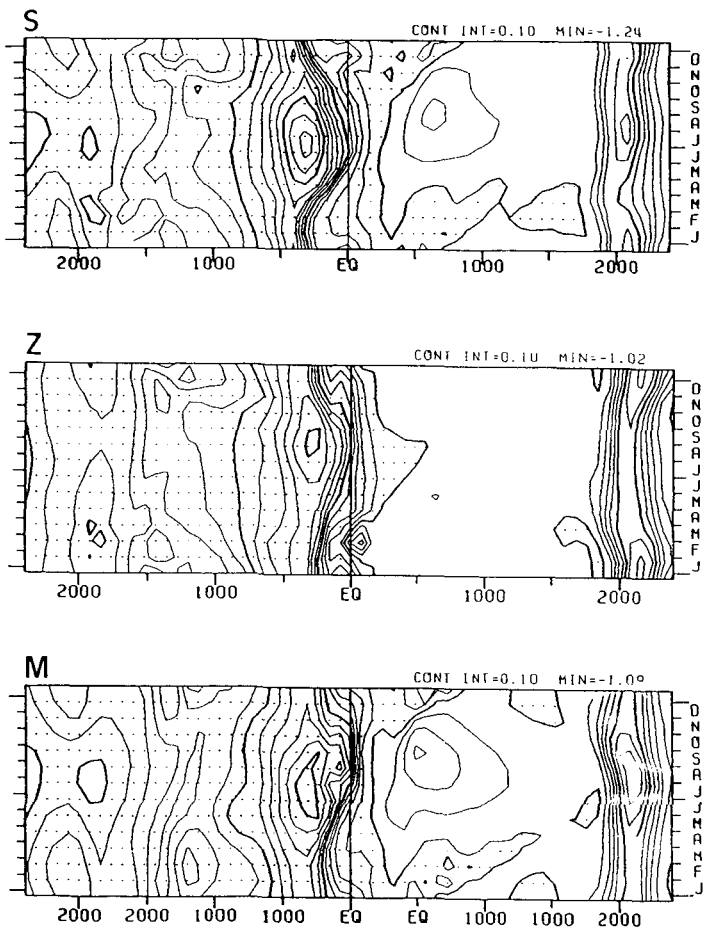

Fig. 13 y-t diagrams of vertical velocity at the bottom of the surface layer along the eastern boundary in Z model and M model compared to the S model.

near the eastern boundary. They are about 3.5℃, 2.3℃ and 1.8℃ for the S, Z and M models, respectively. It means the variation in the S model is not a mere superposition of variations of the other two models, as is expected considering nonlinearity of the process.

Phases of the seasonal variation differ slightly among the models. In the M model, the minimum SST at the eastern boundary occurs about a half month earlier than in the S model, while in the Z model, it delays by a half month. As the direct causes of the seasonal variation of the cold tongue are the coastal upwelling and the zonal surface current along the equator, influences of the absence of the zonal or meridional wind stress component variation on them are of interest. In Fig. 12, it is found that as to the zonal surface current along the equator, the Z model is nearly identical to the S model, while in the M model, seasonal variation is significantly small. For the coastal upwelling along the eastern boundary (Fig. 13), both the Z model and the M model show smaller seasonal variation than the S model. Slight phase differences are found again, this time, the Z model delays by nearly one month to the other models.

5. Summary and conclusion

The main goal of the present study is to throw light on the mechanisms behind the seasonal variation of the cold water tongue in the eastern tropical Pacific Ocean. The cold tongue extends from the South American coast about 7,000 km west along the equator. It is known that in usual years, it is strong from northern summer to fall and weak from winter to spring.

An attempt is made to reproduce the main features of the seasonal variation of the cold water tongue by simple idealized numerical model in which the wind stress is the only external force changing seasonally. The numerical model used here is a 10-level model with rectangular and flat-bottomed model basin. Richardson number dependent mixing coefficients used in Pacanowski and Philander (1981) are employed to parameterized vartical mixing. Sea surface heat flux is parameterized after Haney (1971), and the thermal condition is uniform in time and space near the equator. Seasonal variation of wind stress is idealized as a north-south migration of a trade wind distribution.

The model succeeds to reproduce seasonal variation of the cold water tongue similar to that observed. The phase of the seasonal variation agrees well and an agreement in amplitude is also acceptable. The most serious discrepancy is that in the model distinct SST seasonal variation along the equator can be traced out only about 4,000 km from the eastern boundary, which

is only about a half of the corresponding distance observed. However, overall agreement with observations is good enough to convince us that the mechanism of the seasonal variation of the cold tongue in the model is analogous to that in the real ocean.

Analyses of the model result indicate the following process for the development of the cold warer tongue. The main portion of the cold water tongue is supplied with water mass from the deeper ocean by strong coastal upwelling along thc eastern boundary centered several hundreds kilometers south of the equator in southern winter. Shortly thereafter the upwelled fluid is advected equatorward along the coast, the cold water then extends westward carried by coincidently strong westward current near the equator, in the season from late northern summer to early fall. It is rather surprinsing conclusion that equatorial upwelling does not contribute to the seasonal variation of SST.

As to the relative importance of the coastal upwelling and the equatorial waves, the followings are shown by equatorial wave mode analysis and two additional model experiments in which either one of zonal or meridional component of wind stress is fixed in time. The seasonal variation of the coastal upwelling is due to both variation of local meridional wind stress and remotely forced equatorial Kelvin waves generated by variations of the zonal component of wind stress over the equater, while the variation of the surface current near the equator is attributed mostly to equatorial waves. At any rate, both the locally induced coastal upwelling and the remotely generated equatorial waves contribute to the seasonal variation of the cold water tongue. As is mentioned previously, since the model reproduced the major feature of the seasonal variation of the cold tongue reasonably well, it is expected that the mechanism discussed above explain the phenomenon in the real ocean.

However, precise quantitative discussion is beyond the ability of the present simple model. For that purpose, a more realistic model would be required. In such cases, insufficiency of data for the sea surface heat flux might become a large obstacle. Development of more sophisticated parameterization for vertical mixing should be necessary.

At the same time, it should be emphasized that the seasonal variation of tropical Pacific is so closely related to the interannual variability, especially El Nino events that it is impossible to be understood completely separately. The motivation of the present study came from the idea that it is impossible to understand El Nino events, without knowledge of seasonal variations. The converse is also true, so research on both must advance hand in hand.

Acknowledgement

I am especially grateful to Dr. Antonio J. Busalacchi, for his valuable advice and review of this paper. I would like to acknowledge Dr. James. J. O'Brien for kindly allowing me to use his wind stress data. I would also thanks to miss Chikako Imai, for her help in typing manuscript and preparing figures.

References

Bryan, K., 1969. A numerical method for the study of the circulation of the world ocean. *J. Comput. Phys.*, **4**, 347-376.

Goldenberg, S.B., and J.J. O'Brien, 1981. Time and space variability of tropical Pacific wind stress. *Mon. Wea. Rev.* **109**, 1190-1206.

Haney, R.L., 1971. Surface thermal boundary condition for ocean circulation models. *J. Phys. Oceanogr.*, **10**, 123-1220.

Harrison, D.E., and P.S. Shepf, 1984. Kelvin-wave-induced anomalous advection and the onset of surface warming in El Nino events. *Mon. Wea. rev.* **112**, 923-933.

Horel, J.D. 1982. On the annual cycle of the tropical Pacific atmosphere and ocean. *Mon. Wea. Rev.*, **110**, 1863-1878.

Pacanowski, R., and S.G.H. Philander, 1981. Parameterization of vartical mixing in numerical models of tropical oceans. *J. Phys. Oceanogr.*, **13**, 917-935.

Robinson, M.K., 1976. *Atlas of North Pacific Ocaen monthly mean temperature and mean salinities of the surface layer.* Naval Oceanographic Office, NOO PR-2, 19 pages+ 173figs.